Physically Flexible Ultralow-Power Wireless Sensor

Dung Nguyen, Colm Mc Caffrey, *Member, IEEE*, Olli Silvén, *Senior Member, IEEE*, and Martin Kögler

***Abstract*— The key challenges of local sensor networks are in supporting high sensor density, information security, physical size, and especially energy efficiency at a level that could eliminate the need for batteries or external power supplies. This article presents a novel scheme that answers all issues at the cost of minor information losses in low data rate applications that tolerate latency. Experimental verification is made using a sensor node implemented on a flexible electronics platform. Lightly encrypted data are transmitted by embedding it into Bluetooth advertising packets, contributing to ultralow-energy wireless power consumption, and theoretically enabling an unlimited number of nodes in the local network. In the experiments, the energy dissipation per transmitted 14-B information packet varied between 19.83 and 105.93 μW depending on the system configuration, while the data loss rates ranged from 7.4% to 0.004%, respectively. As the flexible substrate can be attached to various surfaces, the applications extend from wearable to industrial condition monitoring devices.**

***Index Terms*— Flexible printed circuits (FPCs), information security, low-power electronics, wireless sensor networks (WSNs).**

I. Introduction

ENABLING high-density networks of ultralow-power sensors is a persisting challenge. The sensors may measure, for instance, biosignals as wearable devices or monitor mechanical components, such as intelligent strain gauges. In such applications, the designs need to be highly miniaturized and mountable to surfaces of various shapes. These call for technology combinations and solutions that challenge the current state-of-the-art design practices. To answer these needs, in this article, we present a design that is not only flexible to configure and deploy but also physically flexible. The hardware is intended to be a flexible platform that can be adapted for use in a wide range of applications and deployed in a broad number of scenarios. Particular applications' targets include wearables, skin contact and clothing integration, medical, well-being and sports, smart environment, and industrial and environmental monitoring.

The vision of the Internet of Things (IoT) is to sense data in any application and location [1]. The devices needed must possess a small form factor, consume as little power as possible, and should often be bendable or even stretchable. This implies flexible electronics that have become a rapidly evolving market because of the versatility of applications with components on flexible polymeric foils [2]. Applications using flexible designs in consumer electronics, medical and healthcare, automotive, aerospace, and defense industry are estimated to grow with a CAGR of 7.4% from 2020 until 2027 [3] to a global market size of around 42.48 billion USD by the end of 2027. At the same time, awareness of security in IoT is rising with the necessity to add a strong level of data protection on the data collector side [4].

A flexible printed circuit (FPC) is defined as "a patterned arrangement of printed circuitry and components that utilize flexible base material with or without flexible cover lay" [5]. Printed flexible circuits were first described in the literature in 1948 [6] with a suggestion that printed circuits could be made on paper. Recently, there has been a resurgence of paper-based flexible electronics utilizing both inkjet printing [7] and pen-to-paper [8] patterning of conductors.

The current industry standard employs polyimide as the preferred substrate where conductors consist largely of etched rather than printed copper to allow for soldered components. Kapton, one particular polyimide, is the industry standard in flexible circuit fabrication, selected for its excellent durability, stability, and thermal properties [9]. Kapton-based substrates have been effectively used in the 3-D integration of sensor platforms using a folding technique [10].

Advances in flexible circuit technology include flexible thin-film transistors [11]. In the current state of the art, flexible electronics are viewed as a platform technology [12] exploiting recent advances in graphene, nanostructures, and printed conductors that can be manufactured in roll-to-roll (R2R) process [13]. A wide range of applications is described [12], including healthcare, human interactivity, e-textiles, energy, display, and computation.

Flexible hybrid electronics [14] is a new approach aiming to combine the best of both flexible and conventional electronics unlocking significant opportunities while presenting major challenges. Hybrid electronics in the field of wearable technology [15] is a particular area of research interest where physical (temperature, activity, pressure, flow, and light) and chemical (sweat and glucose) parameters can be monitored. Flexible hybrid electronics is especially useful in "beyond wearable" applications where lab-on-skin approaches are being applied to measure biopotentials (ECG, EMG, and EEG), hydration, blood oxygenation, blood pressure, chemical components, and wound monitoring [16].

Along with flexible electronics, the advancement of flexible batteries is also notable. There are many electrode designs each with their own advances and drawbacks [17]. According to recent research [18] a 3.6-V AgO-Zn recharge-

Manuscript received December 17, 2021; revised March 3, 2022; accepted March 14, 2022. Date of publication April 1, 2022; date of current version April 20, 2022. This work was supported by the European Union's Horizon 2020 Research and Innovation Program through the Project Smart and Flexible Energy Supply Platform for Wearable Electronics (Smart2Go) under Grant 825143. The Associate Editor coordinating the review process was Dr. Zhengyu Peng. *(Corresponding author: Dung Nguyen.)*

Dung Nguyen and Martin Kögler are with VTT Technical Research Centre of Finland, 90570 Oulu, Finland (e-mail: nguyenngocquocdung@gmail.com).

Colm Mc Caffrey is with the Device Concept Laboratory, Huawei Technologies Finland Oy, 00180 Helsinki, Finland.

Olli Silvén is with the Center for Machine Vision and Signal Analysis, Faculty of Information Technology and Electrical Engineering, University of Oulu, 90570 Oulu, Finland.

Digital Object Identifier 10.1109/TIM.2022.3164157

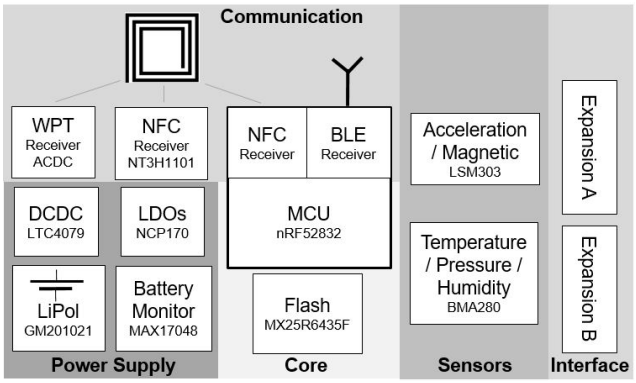

Fig. 1. FlexNode architecture.

able flexible battery can achieve up to 54 mAh/cm^2 with 1-mA constant discharge current and 20-mA peak current, enabling 70-mW momentary dissipation of the powered device.

Cutting the power dissipation not only extends the lifetime of the power source but also allows using low current output flexible batteries or alternative energy sources [19]. Ultralow-power wireless communication on such a flexible sensor platform can be performed when the microcontroller unit (MCU) is capable to wake up only when necessary from sleep-mode or deep-sleep mode [20], [21]. With a low power consumption design, a small energy harvester would be enough to make the system self-powered [22], [23]. Also, designing the embedded software to power down the unnecessary parts of hardware to further reduce energy consumption can decrease the consumption to the μA level.

The functions of an IoT sensor device can be rather simple, i.e., measuring the temperature, humidity, and so on, in a specific place over an extended time. In such cases, bidirectional communications are not necessary since just the sensor data are collected, providing for further opportunity to save energy. Often, these simpler IoT devices are deployed as wireless sensor networks (WSNs), which consists of a group of multiple embedded devices that employ sensors to record the physical conditions of the environment. The most popular architecture is centralized WSN, which has one central unit and many sensing units. In recent years, fog computing and edge computing have gradually been applied to the domain IoT [24].

Wireless communication is responsible for the majority of power dissipation of sensor nodes [25]. In the future, wake-up radio receivers (WURs) would enable turning on the transmitting system only when needed [26], saving substantial energy. However, currently, Bluetooth low energy (BLE) is available in most mobile devices and is one of the lowest energy wireless communication approaches available for wireless sensor designs [27], [28].

II. Materials

The objective of the developed hardware is to enable quick turnaround of implementing IoT concepts for demonstrations and customization for "sensor to the cloud" solutions. As described in Fig. 1, the architecture is divided into four subsections: sensors, processing and communications' core, power supply, and external interface.

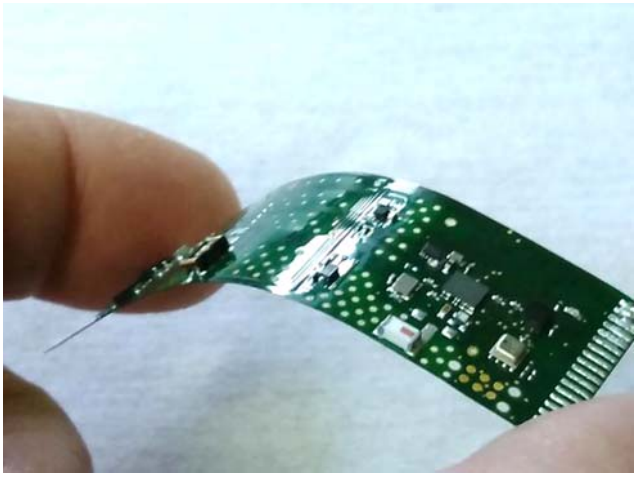

Fig. 2. FlexNode photograph.

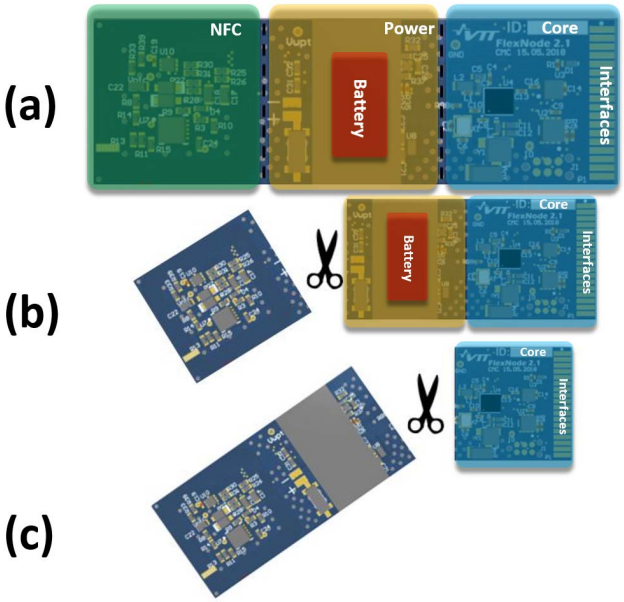

Fig. 3. FlexNode modularity. (a) Full size. (b) NFC cut out. (c) Core, sensor, and expansion port only.

A. Flexible Substrate

A fabricated Flexnode is shown in Fig. 2. To enable this versatility, the key design goals were flexibility and modularity. Physical and mechanical flexibilities are achieved by implementing the hardware on a thin polyimide substrate.

Modularity aims at the capability to scale the functionality of the design based on application needs. In Flexnode, this translates into cutting out unnecessary modules, also reducing the size of the device. Fig. 3(a) shows the full-sized (61 mm $\times$ 19 mm) design. This includes all the functionalities described above.

Fig. 3(b) shows how the rightmost section of the design can be cut out, eliminating the NFC receiver coil that connects to either the nRF or NXP receiver. For applications in which NFC communications and/or wireless charging of the battery are not needed, this gives a 39-mm-long device. A further reduction to 20 mm shown in Fig. 3(c) can be made if an external expansion includes compatible energy storage or harvester.

TABLE I
FLEXNODE COMPONENT SPECIFICATION

Component Name	Description	Specifications	Dimension	Current consumption
nRF52832	Ultra-low power 2 Mbps Bluetooth Low Energy NFC, ANT and 2.4 GHz proprietary SoC	64 MHz ARM Cortex-M4F SPI, I2C, UART 200 kbps ADC	WL-CSP 3 x 3.2 x 0.4 mm	3.7 mA @ 64 MHz 300 nA @ full sleep mode 1.9 µA with RAM retention and Wake-on RTC
MX25R6435F	64 Mbit flash memory Multiple bank	Minimum 100.000 erase/program cycle 20 years data retention	8 pins USON - 4 x 4 mm	7 nA @ Deep Power-down
LSM303	Triple-axis accelerometer and magnetometer Embedded temperature sensor	Accelerometer measure at +/- 2,4,8,16g 1 mg/LBS at 16 bit Magnetic field range +/- 50 gauss 1.5 mgauss/LBS at 16 bit	LGA-12 2 x2 mm	3.7 µA @ 1Hz acceleration sensing 50 µA @ low power magentism
BME280	Temperature, humidity and pressure sensor	Temperature 0-65 °C +/- 1 °C Humidity 0-100 % +/- 3 % Pressure 300-1100 hPA +/- 1 hPA	LGA - 2.5 x 2.5 mm	340, 714 and 350 µA @ high accuracy 1.2, 2.8 and 11 µA @ forced 1 Hz
2450AT18B100E	2.4 GHz chip antenna	Frequency 2400-2500 MHz Impedance 50 Ohm Operating temperature -45 to 125 °C	3.2 x 1.6 x 1.3 mm	Input 2 Watts maximum
NT3H1101	Energy harvesting Field detection and programmable message tag	Operating frequency of 13.56 MHz Data transfer of 106 kbit/s Operating distance of up to 100 mm	LGA - 1.6 x 1.6 x 0.5 mm	155 µA when using I2C

Then, the remaining functionalities include the processing and communications' core, sensors, and expansion ports.

B. Sensors

The selection of the sensor components was motivated by the aim at ultralow-energy dissipation, while the use cases were anticipated to employ low sampling rates. This resulted in the preference for sensors with low-power modes. The key components are summarized in Table I, including their functionalities, specifications, and current consumption from manufacturers' datasheet.

The integrated sensor devices include LGA 12 encapsulated LSM303 [29] which measures three-axis acceleration and a three-axis magnetometer. Also included is a temperature sensor with an accuracy of 1 °C. The other integrated low-power sensor device is 2.5 mm × 2.5 mm LGA packaged Bosch BMA280 [30] environmental sensor, which combines humidity, barometric pressure, and temperature measurements.

C. Processing and Communications' Core and Interfaces

The core of Flexnode is the System-on-Chip Nordic Semiconductors nRF52832 with $3 \times 3.2 \times 0.4$ mm^3 physical dimensions [31]. It contains an ultralow-power ARM Cortex-M4F microcontroller, and 2.4-GHz Bluetooth 5 and ANT/ANT+ radios. For storing functionality, a 64-Mb Macronix MX25R6435F in a 4×4 package is included.

A PI configuration matching network is used to match the RF output to a Johanson 2450AT18B100E chip antenna. The nRF52832 additionally includes a 13.56-MHz NFA Type 1 106-kb/s receiver, which enables "wake-on-NFC" and "touch-to-pair" capabilities. The NFC coil and NXP Semiconductors NTAG NT3H1101 support energy harvesting through NFC, microcontroller interrupt for wake-on-NFC, and I2C interface for communication over NFC. Also, an EEPROM for passive data retention is provided.

Two interface connectors are included for expansion, allowing the addition of further sensing capabilities, or power supplies. The primary interface (Expansion A) is shown on the right edge of the device in Fig. 3. The interface has 18 signals that include both battery and regulated power supplies, ADC inputs, I2C, SPI, and undedicated GPIO pins. For software development and testing, the platform can be connected via this expansion port. The interface (Expansion B) is on the bottom side of the Flexnode and is intended for energy harvester add-ons.

D. Energy Budget and Power Supply

The power supply subsection includes a wireless power transfer receiver and conversion using the NFC coil tuned to series resonance at 13.56 MHz. The wireless power signal from the coil is half-wave rectified and converted for battery charging using an LTC4079.

Energy is currently stored on a 3.7-V Lithium polymer battery measuring $10 \times 20 \times 2$ mm^3 with a 22-mAh capacity. The battery is monitored with a MAX17043 battery-level gauge reporting remaining capacity. The battery voltage is regulated to a stable 2.5 V using an NCP170 linear dropout regulator.

III. FUNCTIONALITY

The FlexNode is intended for uses in which the main need is reading the sensor data and sending it to further processing without being requested and without protocol-level handshakes.

A. Communications

The wireless communications between the Flexnode and receiver (a BLE-enabled laptop) are based on 2.4-GHz BLE radios. While BLE provides for substantial flexibility, in the intended applications, there is no requirement for data streaming or the sensors establishing connections with the hubs.

Flexnode can utilize connection-based BLE protocols for reliable communications; those are reserved for diagnostics and software reconfiguration, and, in the future, for providing public encryption keys.

In the energy minimizing communication scheme developed for Flexnode, only the advertising part of the connection procedure is utilized for data transfers. When comparing the duration of radio communication between connection establishment and advertisement period every 1 or 2 s, the energy efficiency of using advertising packets to transmit small amounts of data is obvious. Furthermore, in the connection data transmission scheme, if the connection is dropped, the effort to reconnect will significantly increase the power consumption.

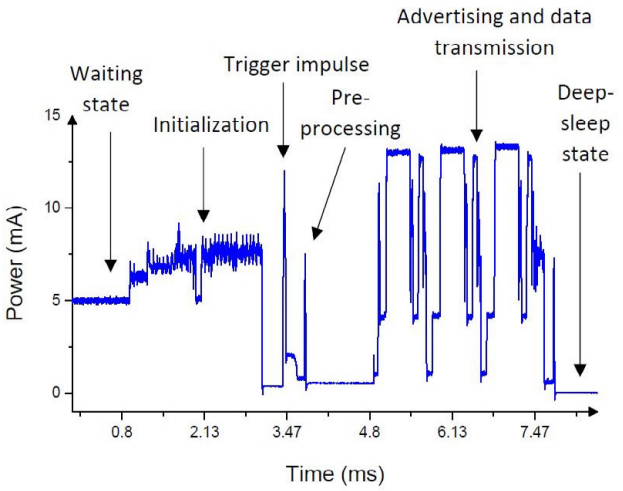

Fig. 4. Advertisement current profile.

To make its presence known to the receivers, a BLE device periodically broadcasts advertising packets in three channels 37, 38, and 39 (2402, 2426, and 2480 MHz), while the remaining channels (0–36) are dedicated to connected protocols. For the communication hubs listening to the advertising channels, this is a one-way discovery mechanism, and it provides Flexnode, a very-low-power means to deliver data.

Fig. 4 shows the current drawn during an advertising event that uses the three channels. The total duration of an advertising event, including the MCU activity, is 3–4 ms, and the advertising interval can be from 20 to 2000 ms. In our case, the peak power dissipation was at a 37.5-mW level. The power consumption of an advertising event is differed by the advertising interval, antenna power, and advertising packet length. A more detailed analysis of the energy impacts of BLE advertising is in [32], while Song *et al.* [33] have introduced a method to optimize its power consumption.

B. Data Packets and Security

The BLE advertising packets comprise at minimum 1 and at most 31 B, as shown in Fig. 5. The first three bytes contain the name of the device, and in our case, the first byte is always the ASCII code "F" (for Flex). The two next ones contain the device number, limiting the theoretical number of devices to 65 535 as device number 0 is not used. In the current application, however, the maximum is 255 to avoid excessive BLE advertising collisions. The extra currently unused device number byte has been considered to be useful for system expansions. Two bytes are for the manufacturer's device ID. In total, 28 B have been left for the free use of the manufacturer. Flexnode uses 1 B for packet ID, and at most 25 B are available for sensing data. In our experiments, only 14 B information packets were used for transmitting temperature, humidity, air pressure, and battery charge level measurements.

Since the bit space in the advertising packet is a significant constraint, the sensor data are transmitted as bit-array. Currently, 3 b are used to identify each of the seven sensors (000 stands for no data, 001 for the combined temperature, humidity and air pressure sensor, and so forth, while the space for data depends on the sensor, for example, 45 b for temperature, humidity, and air pressure). The 200 b are successively filled in this manner and suffice for all the sensors in the current implementation.

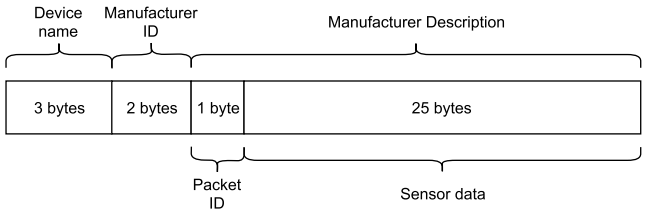

Fig. 5. Advertising packet structure.

TABLE II
BIT ARRAY OF BME 280 DATA

001	0100011111100	00100001001011	010101111110010000
UNIQUE SENSOR ID	13 bits for temperature	14 bits for humidity	18 bits for pressure

TABLE III
ADVERTISING PACKET EXAMPLE

Device Name	Manufacturer ID	Packet ID	Data buffer
F01	0xXX	0xD4	0x2C358709904C4D7D

TABLE IV
DATA ENCRYPTION

Data	2C	35	35	09	90	4C	4D	7D
Key	D5	AB	D5	AB	D5	AB	D5	AB
Result	F9	9E	52	A2	45	E7	98	D6

An example of the sensor data packetizing is shown in Table II. 23.00 °C temperature, 21.23% humidity, and 900-hPa pressure readings are converted into a 45-b section of the array under assembly for transmission. The initial 001 is the identification code of the environmental sensor.

Although the sensor data are in a bit array with different field lengths for each sensor type, it could still be easily decoded by trial and error. To prevent the straightforward misuse of data through eavesdropping BLE receivers, a low-level energy-efficient information obfuscation approach is employed. Its intention is to slightly delay the access of unauthorized parties to the measurements.

The current symmetric encryption scheme employs the 8-b advertising packet number as the key. XOR between each packet number and the second byte of device ID generates a changing XOR cipher that is renewed for every new packet with the bits of the cipher used in alternating order depending on the packet number. A simple example of this energy-efficient scheme is described in Table III.

The key is calculated as 0×01 XOR $0 \times D4 = 0 \times D5$, so the bit reversed key is $0 \times AB$. As the device ID is "1" (F01), we XOR the first, third, fifth, and seventh bytes with $0 \times D5$ and the other bytes with $0 \times AB$. This encryption procedure is described byte-by-byte in Table IV. The data buffer in the advertising packet becomes the encrypted byte array $0 \times F99E52A245E798D6$.

TABLE V
EVALUATE DEVICES SETTINGS

Local Name	F01	F02	F03
MAC Address	C1:85:6B:55:8E:BF	D7:51:AD:92:6C:D6	E5:B5:04:14:42:BF
Advertising Interval	500 ms	625ms	125ms
Advertising Timeout	5 seconds	5 seconds	20 seconds
Advertising packets/period	10 packets/period	8 packets/period	160 packets/period
Number of enabled sensors	BME280 – always enabled MAX17043 – once every 10 events	2 sensors always enabled	2 sensors always enabled

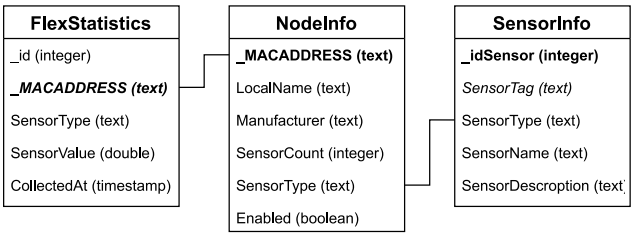

Fig. 6. Database design.

While the approach provides for a fairly low level of information security, it may suffice for noncritical applications. However, through brute force effort, an attacker knowing the bit allocation scheme can check if a deciphered result could be correct.

Employing a more powerful public-key encryption scheme is a future alternative. While the short bit length reserved for data does not allow for high-level security, new keys could be provided through BLE connections for each device.

IV. EXPERIMENTS AND RESULTS

A. Evaluation Procedure

To evaluate the Flexnode implementation, a Windows PC software application for Bluetooth scanning and database has been employed. Fig. 6 shows that the data tables model the network and the sensors. The information of the sensors and nodes is in SensorInfo and NodeInfo, respectively, while FlexStatistics contains all data collected from the sensors and nodes, enabling to track the source and time of each measurement.

The multithreaded PC application is developed using the Microsoft .NET framework. Three threads run simultaneously: Scanning and Data Collecting run always in the background, while the Discover Thread is launched whenever the user wants to add new nodes into the network. The advertising packets of the devices in the database are collected and queued by the Scanning Thread. Each packet is, in turn, decoded and stored to the FlexStatistics by the Data Collecting Thread. The internal organization of the application is shown in Fig. 7.

The experimental network used to determine the energy characteristics of the Flexnode design consists of three devices identified as F01, F02, and F03, a laptop PC collecting the statistics, and running the application. The nodes were configured to transmit advertising packets at different rates, going to sleep between transmissions, to gain a concrete understanding of the impact on the endurance. The nodes were powered by two Varta Ultra Lithium AA batteries having 2900-mAh capacity.

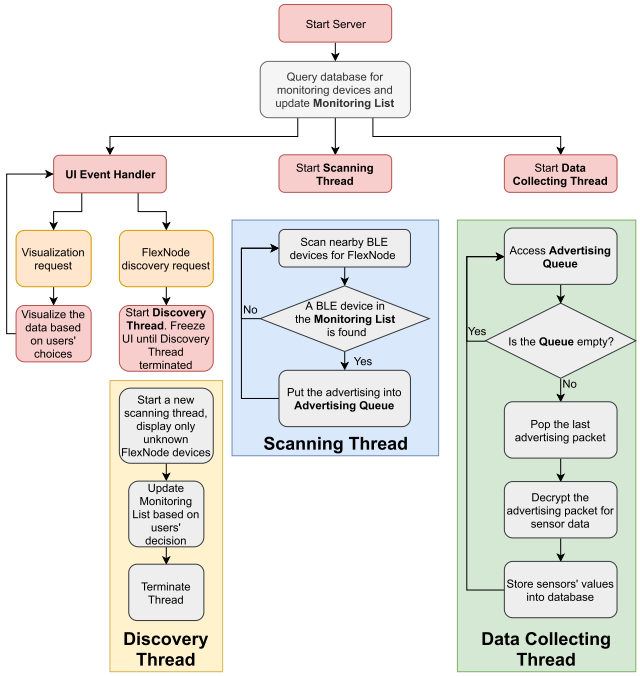

Fig. 7. Server flowchart.

TABLE VI
POWER CONSUMPTION SUMMARY

FlexNode	F01	F02	F03
Voltage Dropped	71 mV	45 mV	152 mV
Data Lost	5.8 %	7.4 %	0.004 %
Avg. Current	8.78 μA	7.93 μA	42.35 μA
Power consumption	21.95 μW	19.83 μW	105.93 μW

The settings of each device are given in Table V. The system was consecutively run running for 48 days.

B. Results

Based on the experiment, the packet loss rates of nodes F01 and F02 were 5.8% and 7.4%, respectively, while F03 suffered only 0.004% loss. The battery voltages of the FlexNodes dropped less than 200 mV during the 48-day test. The most energy-hungry one, F03, experienced a 152-mV drop, while F02 used its battery most conserving losing only 45 mV. Table VI describes the voltage drop and power consumption of the three nodes.

Based on the current waveform analyzer (CX3324A, Keysight Technologies), the power on sleep-mode current need of Flexnode is 3.7 μA and, in the active sensing mode, about 1.4 mA for a very short time, about 300 μs. The current consumption during transmission depends on the number of advertising packets in advertising events.

Node F03 had the most power-consuming settings with average current consumption during transmission at 100.3 μA. Consequently, its average power dissipation is

$$I_{\text{avg}} = \frac{I_{\text{active}} * t_{\text{active}} + I_{\text{sleep}} * t_{\text{sleep}} + I_{\text{process}} * t_{\text{process}}}{T_{\text{total}}} \quad (1)$$

where I_{active} and t_{active} are the BLE advertising current and time; I_{sleep} and t_{sleep} are the current and time between two advertising event; I_{process} and t_{process} are the current and time for data processing; and T_{total} is the total time for one cycle [34]. The average current can be obtained by substituting the measured values into 1

$$\frac{3.7\ \mu\text{A} * 30\ \text{s} + 100.3\ \mu\text{A} * 20\ \text{s} + 1400\ \mu\text{A} * 0.0003\ \text{s}}{50.0003\ \text{s}} = 42.35\ \mu\text{A}. \quad (2)$$

From a 2000-mAh battery at 70% efficiency, the node will run for over 30 000 h or 3.5 years.

If the power supply module is an organic photovoltaic (PV) harvester, the size of the cell is

$$A = \frac{E_{\text{electrical}}}{H * R * \text{PV}_{\text{efficiency}}} \quad (3)$$

where

A: area of PV Panel;
$E_{\text{electrical}}$: energy required;
H: annual average solar radiation on tilted panels -200 kWh/m^2/year;
R: solar panel yield or efficiency 15%;
$\text{PV}_{\text{efficiency}}$: performance ratio, coefficient for losses -0.75.

In theory, the system could become completely autonomous that would not require any battery replacement with an about 1.5-cm^2 PV cell minimum size. However, with the current power supply hardware, it supports adjustable battery charging current to operate from 10 to 250 mA.

V. Discussion

The aim of this contribution is to present an energy-autonomous wireless sensor platform that can be used from industrial condition monitoring instruments to wearable human biosignal measurements devices. The energy consumption has been minimized by employing BLE advertising packets for data transmission. This not only reduces the energy consumption of the radio but eliminates almost all protocol complexity. While the lack of protocol connection results in data losses, many applications can tolerate moderate ones. Furthermore, if the nodes of the network are known, the server side is capable of detecting failed nodes or excessive data loss rates.

For a particular application, the physically flexible platform that allows for cutting out redundant parts enables minimizing the size and weight of the sensor node. The experimental sensor nodes were tested continuously for more than a month and a half without hardware or software complications.

The system design suits applications that have low data rates and benefit from light, small, and thin sensor nodes in low and medium ranges. These include, for example, monitoring the minimum and maximum vibrations of industrial motors or the temperature threshold of cylindrical objects, such as shafts.

TABLE VII
Power Consumption Comparison

ZigBEE	treNch	Our proposal
14 µW in sleep mode 31 mW in TX mode	5.4 µW in sleep mode 9.8 mW TX from sleep mode	11.1 µW in sleep mode 0.3 mW during advertising

However, for the application that requires data transmission through extended distances, the Long Range Wide Area Network (LoRaWAN) is the most compatible approach [35].

The selection of the hardware components, including the sensors and the communications scheme, plays an important role in power dissipation minimization. The Nordic Semiconductor nRF52 series with the Arm Cortex M4 processor is among the best low-power system chips that incorporate 2.4-GHz radio. A power consumption comparison between our solution against the roughly equivalent ones cited in this article is given in Table VII. In the scope of this article, we demonstrate a simple but effective encryption method targeting to minimize power consumption, but the chip is capable of using a stronger encryption algorithm with more power and time needed.

The Flexnode platform has many extension pins that can be used to connect sensors, energy harvesters' actuators, and indicators. The future enhancements will include plug-and-play functionality for the extensions, e.g., through the utilization of I2C protocol chip addresses. Moreover, as an I2C channel can support multiple sensors, the complexity of the platform design would be well controlled. Also, an energy monitoring scheme needs to be implemented to allow balancing the use of sensors against the energy being harvested.

VI. Conclusion

In many applications, the thickness, size, and flexibility of the physical platform are important. The current contribution demonstrates not only those characteristics but also wireless energy-efficient data communications in such a system. The platform can be expanded with additional sensors and energy harvesters to fit the requirements of relevant applications. With the capability of extending sensor and platform flexibility, this platform can be applied to wearable, bendable, rollable use cases with extension platforms, such as sweat analytics and ECG/PPG measurement.

Many monitoring needs do not require high data rates. The demonstrated novel low data bandwidth communication scheme is compatible with common standards, enabling to access sensor nodes even using a regular cell phone with BLE.

Conflict of Interest

The authors declare to have no known competing financial or any conflict of interests that would have given influence to the work presented in this article.

References

[1] M. Bhagat, D. Kumar, and S. M. Balgi, "Application of Internet of Things in digital pedagogy," in *Computational Intelligence in Digital Pedagogy*. Cham, Switzerland: Springer, 2021, pp. 219–234.

[2] B. Rivkin *et al.*, "Shape-controlled flexible microelectronics facilitated by integrated sensors and conductive polymer actuators," *Adv. Intell. Syst.*, vol. 3, no. 6, Jun. 2021, Art. no. 2000238.

[3] R. Humbare, S. Wankhede, and V. Kumar, "Flexible electronics market by component and application: Global opportunity analysis and industry forecast, 2020–2027," Allied Market Res., Portland, OR, USA, Tech. Rep. A00850, Nov. 2020. [Online]. Available: https://www.alliedmarketresearch.com/flexible-electronics-market

[4] M. B. M. Noor and W. H. Hassan, "Current research on Internet of Things (IoT) security: A survey," *Comput. Netw.*, vol. 148, pp. 283–294, Jan. 2019.

[5] *Terms and Definitions for Interconnecting and Packaging Electronic Circuits, Revision F*, document IPC-T-50, 1996.

[6] C. Brunetti and R. W. Curtis, "Printed-circuit techniques," *Proc. IRE*, vol. 36, no. 1, pp. 121–161, Jan. 1948.

[7] Z. Zhang, X. Zhang, Z. Xin, M. Deng, Y. Wen, and Y. Song, "Synthesis of monodisperse silver nanoparticles for ink-jet printed flexible electronics," *Nanotechnology*, vol. 22, no. 42, Oct. 2011, Art. no. 425601.

[8] A. Russo, B. Y. Ahn, J. J. Adams, E. B. Duoss, J. T. Bernhard, and J. A. Lewis, "Pen-on-paper flexible electronics," *Adv. Mater.*, vol. 23, no. 30, pp. 3426–3430, 2011.

[9] Q.-H. Lu and F. Zheng, "Polyimides for electronic applications," in *Advanced Polyimide Materials*. Amsterdam, The Netherlands: Elsevier, 2018, pp. 195–255.

[10] R. V. Martinez-Catala and J. Barrett, "A modular wireless sensor platform with fully integrated battery," *IEEE Trans. Compon. Packag. Technol.*, vol. 32, no. 3, pp. 617–626, Sep. 2009.

[11] K. Myny, "The development of flexible integrated circuits based on thin-film transistors," *Nature Electron.*, vol. 1, p. 30, Jan. 2018.

[12] A. Nathan *et al.*, "Flexible electronics: The next ubiquitous platform," *Proc. IEEE*, vol. 100, no. 5, pp. 1486–1517, May 2012, doi: 10.1109/JPROC.2012.2190168.

[13] T. M. Kraft, L. Leppanen, T. Kololuoma, S. Lahokallio, L. Frisk, and M. Mantysalo, "High density R2R screen printed silver interconnections for hybrid system integration," in *Proc. 6th Electron. Syst.-Integr. Technol. Conf. (ESTC)*, Sep. 2016, pp. 1–6.

[14] G. Tong, Z. Jia, and J. Chang, "Flexible hybrid electronics: Review and challenges," in *Proc. IEEE Int. Symp. Circuits Syst. (ISCAS)*, May 2018, pp. 1–5.

[15] W. Gao, H. Ota, D. Kiriya, K. Takei, and A. Javey, "Flexible electronics toward wearable sensing," *Acc. Chem. Res.*, vol. 52, no. 3, pp. 523–533, Mar. 2019.

[16] Y. Liu, M. Pharr, and G. A. Salvatore, "Lab-on-skin: A review of flexible and stretchable electronics for wearable health monitoring," *ACS Nano*, vol. 11, no. 10, pp. 9614–9635, 2017.

[17] Y. Zhao and J. Guo, "Development of flexible Li-ion batteries for flexible electronics," *InfoMat*, vol. 2, no. 5, pp. 866–878, Sep. 2020.

[18] L. Yin *et al.*, "High performance printed AgO-Zn rechargeable battery for flexible electronics," *Joule*, vol. 5, no. 1, pp. 228–248, Jan. 2021.

[19] J. D. MacKenzie and C. Ho, "Perspectives on energy storage for flexible electronic systems," *Proc. IEEE*, vol. 103, no. 4, pp. 535–553, Apr. 2015.

[20] M. Losada, A. Cortés, A. Irizar, J. Cejudo, and A. Pérez, "A flexible fog computing design for low-power consumption and low latency applications," *Electronics*, vol. 10, no. 1, p. 57, Dec. 2020.

[21] O. Kanoun *et al.*, "Energy-aware system design for autonomous wireless sensor nodes: A comprehensive review," *Sensors*, vol. 21, no. 2, p. 548, Jan. 2021.

[22] E. Sardini and M. Serpelloni, "Self-powered wireless sensor for air temperature and velocity measurements with energy harvesting capability," *IEEE Trans. Instrum. Meas.*, vol. 60, no. 5, pp. 1838–1844, May 2011.

[23] M. D. Prieto, D. Z. Millan, W. Wang, A. M. Ortiz, J. A. O. Redondo, and L. R. Martinez, "Self-powered wireless sensor applied to gear diagnosis based on acoustic emission," *IEEE Trans. Instrum. Meas.*, vol. 65, no. 1, pp. 15–24, Jan. 2016.

[24] B.-Y. Ooi and S. Shirmohammadi, "The potential of IoT for instrumentation and measurement," *IEEE Instrum. Meas. Mag.*, vol. 23, no. 3, pp. 21–26, May 2020.

[25] M. A. Nasab, S. Shamshirband, A. Chronopoulos, A. Mosavi, and N. Nabipour, "Energy-efficient method for wireless sensor networks low-power radio operation in Internet of Things," *Electronics*, vol. 9, no. 2, p. 320, Feb. 2020.

[26] F. Hutu, A. Khoumeri, G. Villemaud, and J.-M. Gorce, "A new wake-up radio architecture for wireless sensor networks," *EURASIP J. Wireless Commun. Netw.*, vol. 2014, no. 1, pp. 1–10, Dec. 2014.

[27] F. Moreno-Cruz, V. Toral-López, A. Escobar-Molero, V. U. Ruíz, A. Rivadeneyra, and D. P. Morales, "TreNch: Ultra-low power wireless communication protocol for IoT and energy harvesting," *Sensors*, vol. 20, no. 21, p. 6156, Oct. 2020.

[28] K. Nair *et al.*, "Optimizing power consumption in IoT based wireless sensor networks using Bluetooth low energy," in *Proc. Int. Conf. Green Comput. Internet Things (ICGCIoT)*, Oct. 2015, pp. 589–593.

[29] *Ultra-Compact High-Performance eCompass Module: Ultra-Low-Power 3D Accelerometer 3D Magnetometer*, ST Microelectronics, Geneva, Switzerland, 2016.

[30] *Combined Humidity Pressure Sensor*, Bosch, Gerlingen, Germany, 2014.

[31] *nRF52832 Product Specification*, Nordic Semiconductors, Oslo, Norway, 2017.

[32] C. Gomez, J. Oller, and J. Paradells, "Overview and evaluation of Bluetooth low energy: An emerging low-power wireless technology," *Sensors*, vol. 12, no. 9, pp. 11734–11753, 2012.

[33] S. W. Song, Y. S. Lee, F. Imdad, M. T. Niaz, and H. S. Kim, "Efficient advertiser discovery in Bluetooth low energy devices," *Energies*, vol. 12, no. 9, p. 1707, May 2019.

[34] S. K. Gharghan, R. Nordin, and M. Ismail, "Energy efficiency of ultra-low-power bicycle wireless sensor networks based on a combination of power reduction techniques," *J. Sensors*, vol. 2016, pp. 1–21, Jul. 2016.

[35] L. G. Manzano *et al.*, "An IoT LoRaWAN network for environmental radiation monitoring," *IEEE Trans. Instrum. Meas.*, vol. 70, pp. 1–12, 2021.

Dung (Daniel) Nguyen received the B.Sc. degree in computer engineering from Vietnam National University, Hanoi, Vietnam, in 2012, and the M.Sc. degree in computer science and engineering from the Faculty of Information Technology and Electrical Engineering, University of Oulu, Oulu, Finland, in 2019.

He is currently working as the Research Scientist of the Flexible Electronics Integration Research Team, VTT Technical Research Centre of Finland, Oulu. His research focus is on smart embedded software and electronics design.

Colm Mc Caffrey (Member, IEEE) received the B.Eng. degree (Hons.) in electronic engineering and the M.Eng.Sc. degree in microelectronics from University College Cork, Cork, U.K., in 2006 and 2008, respectively.

He has worked as an Intern Application Engineer with Analog Devices, Wilmington, MA, USA, from 2005 to 2006; a Graduate Researcher and an Instrumentation Engineer with the Tyndall National Institute, Cork, from 2006 to 2010; the Research Scientist of VTT Technical Research Centre of Finland, Espoo, Finland, from 2012 to 2019; and the Senior Scientist of VTT Technical Research Centre of Finland from 2019 to 2021, where this work was carried out. Since 2021, he has been working as a Principal Engineer and a Wearable Prototype Architect with Huawei Technologies Finland Oy, Helsinki, Finland.

Olli Silvén (Senior Member, IEEE) is currently a Professor of signal processing engineering with the University of Oulu, Oulu, Finland. His current research interests range from environment wireless self-powered vision sensors to embedded machine learning in diverse applications. His past contributions include solutions for industrial visual inspection systems to video codecs.

Martin Kögler received the Dr.Ing. degree from the Technical University of Berlin, Berlin, Germany, in 2018.

Since then, he has been working as the Senior Scientist of VTT Technical Research Centre of Finland, Oulu, Finland, in the field of sensing and integration. Apart from customer contract research, his focus area and research interests are applied sensor technologies, electronics integration, and data analytics. His work at VTT includes strong collaboration with various customers and research institutes across the globe.